

EBSD Analysis of Nugget Zone in Dissimilar Friction Stir Welded AA2024-AA7075 Joint Along Weld Thickness

Zhang Chenghang, Huang Guangjie, Cao Yu, Li Wei, Liu Qing

Chongqing University, Chongqing 400044, China

Abstract: The plates of AA2024-T351 and AA7075-T651 with 5 mm in thickness were butt joined by friction stir welding. The microstructural evolution of the nugget zone (NZ) in the dissimilar AA2024-7075 joints along the thickness direction was studied by the method of EBSD. The results indicate that the grain size of the NZ decreases from the top to the root of the joint. The fraction of dynamic recrystallization in the shoulder affected zone (SAZ) and the weld bottom is lower than that in the center of the NZ. Simple shear texture can be developed in the NZ and the texture distributions are heterogeneous. The SAZ consists of B and \bar{B} components, while A or \bar{A} components are the major textures at the bottom. C component is found in the middle of the NZ. The texture intensity in the middle of the NZ is lower than that at the top and bottom. This is mainly due to the presence of the onion ring, in which materials mixing occurs, resulting in a more random grain orientation.

Key words: aluminum alloys; friction stir welding; microstructure; texture

Welding of dissimilar aluminum alloys is difficult via traditional fusion process, which is attributed to not only the difference in physical, mechanical and chemical properties of the two materials, but also to some defects (e.g. cracks and voids) caused by fusion process^[1]. Friction stir welding (FSW) is an innovative solid state joining technique, since the materials being welded do not melt and solidify during FSW, which has been illustrated particularly suitable for the joining of high strength aluminum alloys^[2]. Generally, the FSW joint can be divided into three regions: the nugget zone (NZ), the thermos-mechanically affected zone and the heat-affected zone. The NZ is prone to experience dynamic recrystallization process and obtain a fine and equiaxed grains structure, owing to the influence of strongly mechanical stirring and high heat input^[3,4].

Many researchers have studied the microstructure and texture evolution in similar and dissimilar joints of heat treatable aluminum alloys^[5-11]. Xu et al^[7] investigated that the texture transition and its corresponding activation of $\{111\}$ slip contributes to the recrystallization, which demonstrates

that grain refinement of NZ is facilitated by the $\langle 111 \rangle // ND$ fiber textures in the AA7075 joint. Imam et al^[8] reported that B/B texture component is dominated at the top of the NZ, while the $\{111\} \langle 112 \rangle$ components of A fiber and C component of B fiber are formed at the bottom of the NZ in the AA6063 joint. Wang et al^[10] found that the $\{001\} \langle 100 \rangle$ Cube, $\{123\} \langle 634 \rangle$ S components of the base metal can be gradually transformed into $\{111\} \langle 112 \rangle$ shear texture in the AA5052 and AA6061 dissimilar joint. Thus, it can be concluded that some obvious differences may be observed in the characterization of microstructure and crystallographic on both the advancing side (AS) and retreating side (RS) of FSW joints, especially for dissimilar joints.

So far, a lot of work has been performed on the FSW technique of dissimilar heat treatable aluminum joints. However, few attempts were reported to study the microstructure and crystallography texture through thickness of AA2024 and AA7075 dissimilar joint. Consequently, the microstructure and texture characteristics of the dissimilar AA2024-7075 joint were investigated by the method of

Received date: October 18, 2018

Foundation item: Fundamental Research Funds for the Central Universities (106112015CDJXY130003, 106112015CDJXZ138803); National Natural Science Foundation of China (51421001)

Corresponding author: Huang Guangjie, Ph. D., Professor, College of Materials Science and Engineering, Chongqing University, Chongqing 400044, P. R. China, Tel: 0086-23-65112334, E-mail: gjhuang@cqu.edu.cn

Copyright © 2019, Northwest Institute for Nonferrous Metal Research. Published by Science Press. All rights reserved.

electron backscattered diffraction (EBSD) in the present study.

1 Experiment

AA2024-T351 and AA7075-T651 sheets with a dimension of 300 mm × 40 mm × 5 mm were butt-welded by FSW perpendicular to the rolling direction (RD). The AA2024 and AA7075 sheets specimens were placed on the AS and RS, respectively. The tool was used by a conical thread probe with 3.76 mm in tip diameter and 5 mm in length as well as a concave shoulder of 15 mm in diameter. The tool tilt was 2.5°. A large number of welding experiments have been conducted, and the optimal combination welding parameters with a rotational speed of 1495 r/min and a welding speed of 187 mm/min were used for FSW.

The specimens for metallographic examination were polished and etched using Keller's reagent and then observed on an optical microscope (OM, Zeiss-Axiovert 40 MAT). EBSD analysis was conducted to study both the microstructure and texture along weld thickness of the joints as shown in Fig.1. Here, ANZ and RNZ means the NZ towards AS and RS, respectively. CNZ refers to the center of the NZ. EBSD images were acquired using a scanning electron microscope (SEM, TESCAN MIR3) equipped with a HKL-EBSD system and the step size of EBSD scanning was 0.3 μm. The samples for EBSD were mechanically ground and electro-chemically polished in a solution of perchloric acid and alcohol (1:9) at 15 V and 2 °C for 120 s. All EBSD data were analyzed using the Channel 5 software.

2 Results and Discussion

2.1 Optical micrographs in the NZ of the joint

Fig.2 shows optical microstructure of different zones along the weld thickness direction in the NZ. It can be observed that the microstructure distribution is inhomogeneous in the NZ, which contains two types of materials from the two base materials (BMs). As shown in Fig.2a, the top of the NZ is shoulder affected zone (SAZ). There exists a mixing between the two base materials to some extent. Banded structure and onion ring are observed in the middle of the NZ in Fig.2b and 2c. The bottom areas in the NZ (Fig.2d) mainly come from the BM on the AS.

2.2 Grain structure development

The initial grain structures of the two BMs are displayed in Fig.3. The high angle grain boundaries (HAGBs) with the misorientation angle over 15° are shown by black lines, while low angle grain boundaries (LAGBs) in the range of 2°~15° are presented as white. As seen in Fig.3a and 3b, the grain structures of the BMs are characterized by some elongated grains. The misorientation angle distributions in Fig.3c demonstrate that a large number of HAGBs (~85.6%) exist in the AA2024-T351 and LAGBs (~67.2%) present in the AA7075-T651.

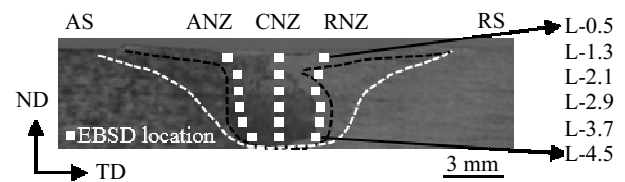


Fig.1 Macroscopic photograph of the dissimilar joint

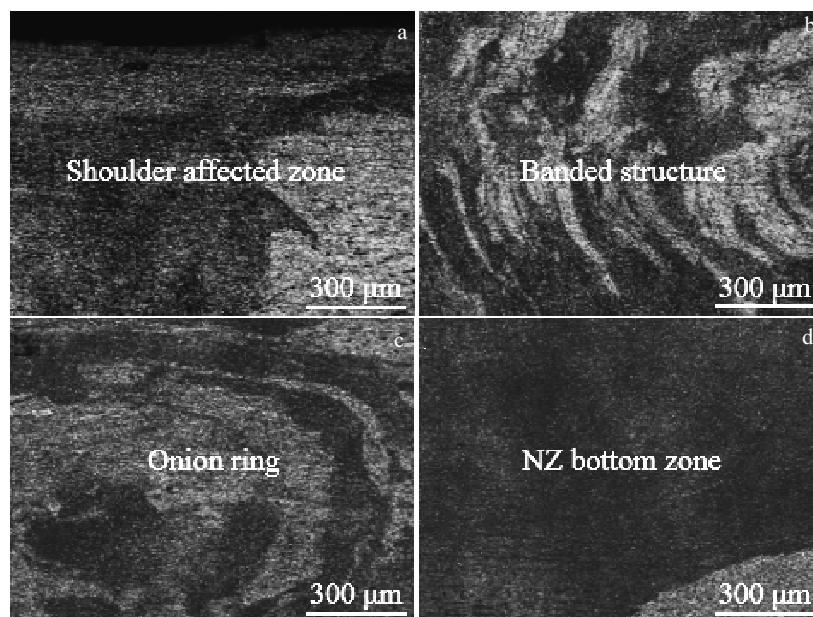


Fig.2 Metallographic structure in the top (a), the middle (b, c) and the bottom (d) of the NZ in the joint

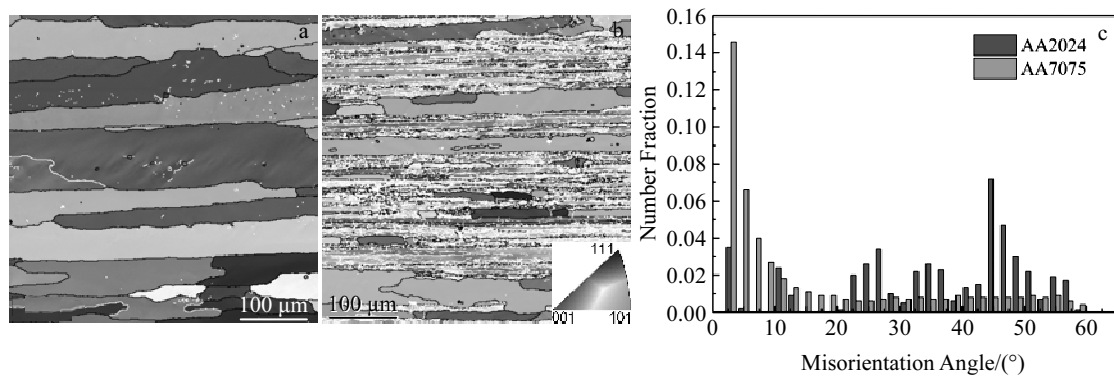


Fig.3 Grain structure of BMs: (a) AA2024, (b) AA7075, and (c) the misorientation angle distribution of the two BMs

Fig.4 shows the grain structure in the ANZ, CNZ and RNZ with different depths. It is obvious from the figure that all of the measured regions display fine grain structures, which is a typical feature of dynamic recrystallization. The material will experience strong mechanical stirring and thermal cycle during the process of FSW, which leads to the formation of fine equiaxed grains.

The average grain size was estimated by EBSD at all the locations of NZ and the results are illustrated in Fig.5. It can be observed that the average grain size gradually decreases along the direction of weld thickness from the top to the bottom in the ANZ, CNZ and RNZ. Apparently, a coarser grain structure can be observed at the top of ANZ (3.8 μm at the position of L-0.5), which is most likely owing to the additional heating by friction between the shoulder and materials surface, adding for extra heating time during the thermal cycle of FSW. The larger grains at the top in the CNZ and RNZ arise from the

insufficient materials flow in the SAZ (Fig. 2a).

It is obviously observed from Fig.4 and Fig.5 that the grain size at the weld bottom (1.2 μm at the position of L-4.5) is lower than that of other locations. Xu et al^[12] found that the temperature gradually decreases from the top surface to the bottom in the weld and the peak temperature difference through the thickness is over 20 °C. Canaday et al^[13] reported that the peak temperature difference is large from the top to the bottom of the NZ with increasing the thickness of the sheet. The material in the weld root is only stirred by the pin, which results in inadequate deformation and lower heat input. Moreover, the heat loss is much more due to the interface between the backing plate and the root surface of the plate. Accordingly, insufficient deformation and low peak temperature would lead to a lower grain size in the weld bottom.

The recrystallization fraction (RF) at various depths in the NZ is depicted in Fig.6. The RF maps were automatically

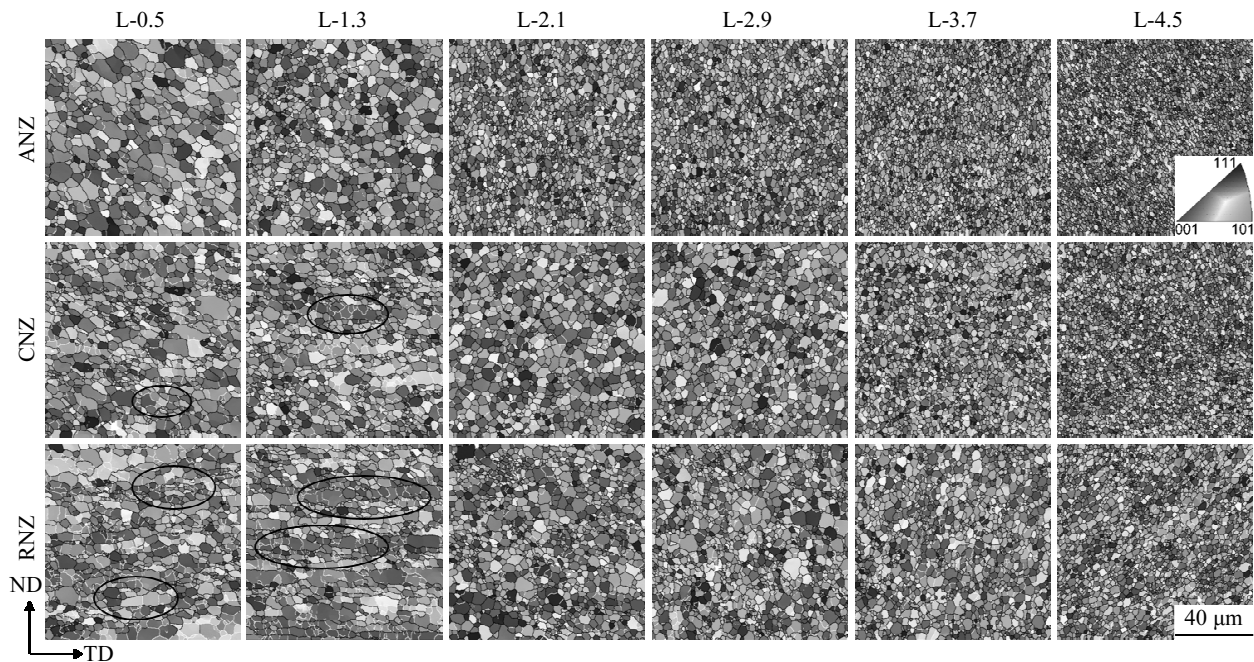


Fig.4 Grain structure variation along the weld thickness in the ANZ, CNZ, and RNZ

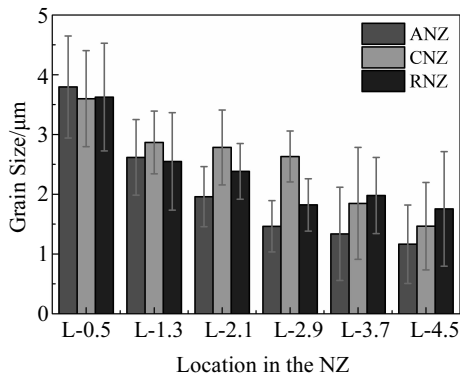


Fig.5 Average grain size of the different locations in the NZ

generated in the Tango module on internal average misorientation (IAM) of individual grains, by first establishing the grains on the basis of the pre-established HAGBs and later by calculating the IAM inside each grains. Then a grain with $IAM > 2^\circ$ was classified as deformed grain, while that without LAGBs and with $IAM < 2^\circ$ was classified as recrystallized grain. A substructured grain comprised of subgrains with $IAM < 2^\circ$ and inter-subgrain misorientation $> 2^\circ$. Obviously, the RF within the shoulder zone (L-0.5, L-1.3) is lower than that of other locations. This may be attributed to inadequate materials flow (Fig.2a) though experiencing high heat input. The

original grains in the SAZ are heavily distorted by the tool shoulder and their remnants contain abundant LAGBs, leading to a lower RF. Conversely, in the middle of the NZ (L-2.1, L-2.9), this region undergoes sufficient materials flow and high heat input, leading to a higher RF. At the bottom, lower temperature may result in a lower RF.

2.3 Misorientation distribution

Fig.7 exhibits the misorientation distribution of NZ with different depths. It is clearly observed that a lot of LAGBs present in the location L-0.5 and L-1.3 when compared to other locations in the NZ, which subdivides the bulk grains into very small subgrains as indicated by black oval in Fig.4. In general, the subgrains can be generated by static recovery during annealing at moderate temperatures for cold-deformed metallic materials or by dynamic recovery during cold to hot deformation of metallic materials with high stacking fault energy. The temperature field is usually depicted as a distorted ellipse described by isothermals of higher temperature in the FSW, in which the initial deformation takes place at low to medium temperatures. Accordingly, the initial dislocations and the dislocations caused by the plastic deformation can be accumulated and rearranged into LAGBs by static or dynamic recovery, which eventually results in the formation of subgrains.

2.4 Texture inhomogeneity

Fig.8 shows the micro-textures at the different positions of

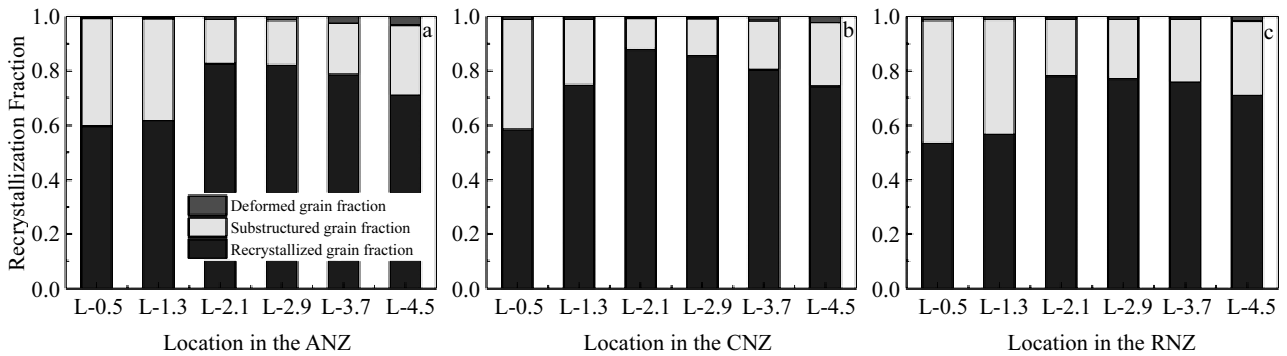


Fig.6 RF at the different locations in the ANZ (a), CNZ (b), and RNZ (c)

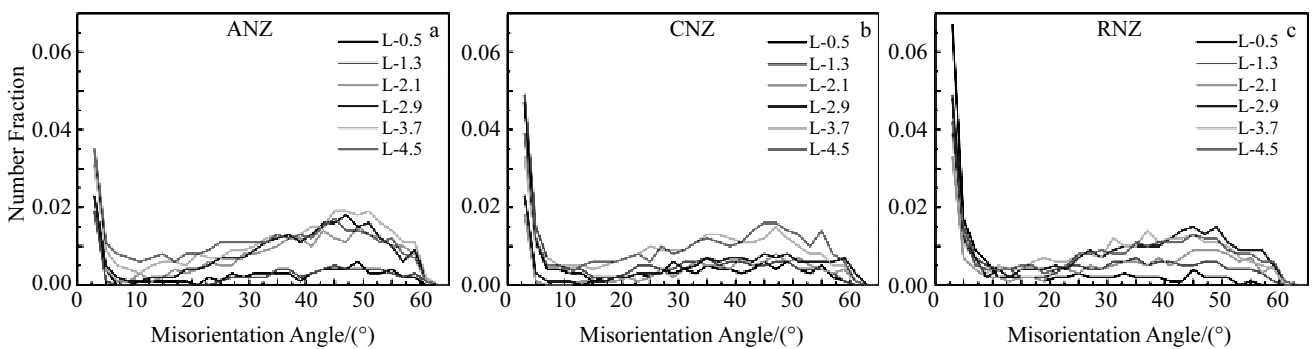


Fig.7 Misorientation angle distribution in the ANZ (a), CNZ (b), and RNZ (c)

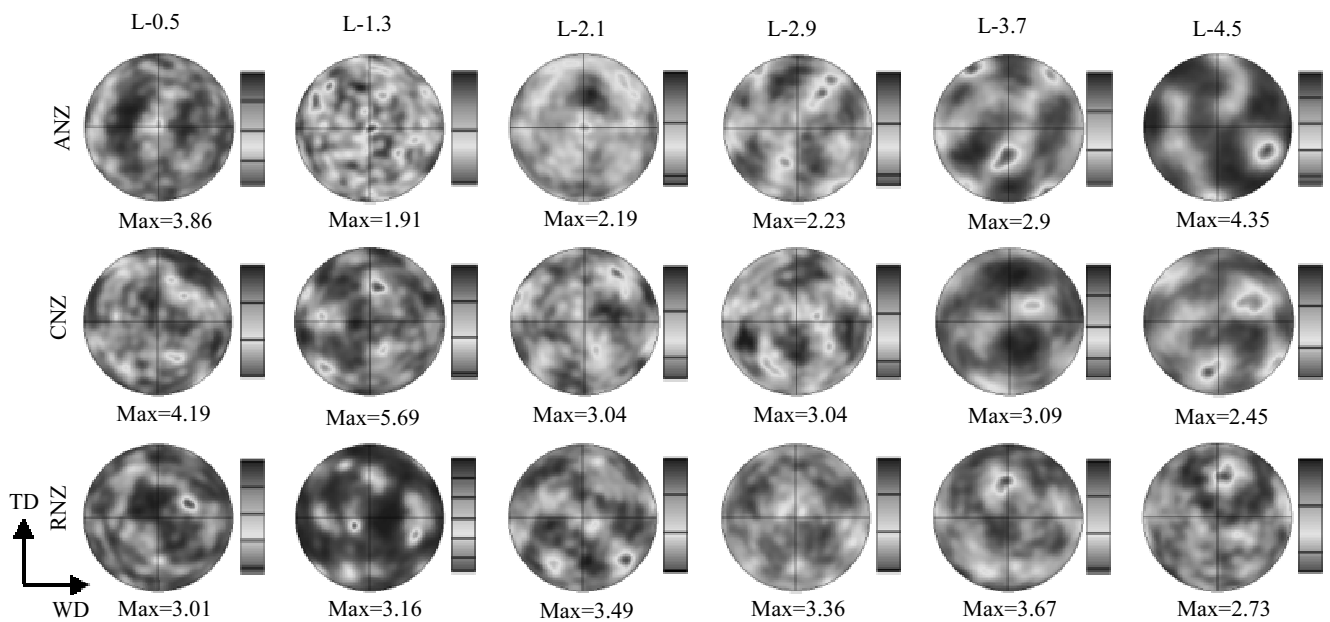


Fig.8 {111} pole figures at the different locations of the NZ along the weld thickness direction

the NZ along the weld thickness. Each of the pole figures was acquired by the EBSD measurements corresponding to the locations illustrated in Fig.1. It is clearly observed that a typical shear texture can be found at the NZ of the dissimilar joint as documented in the previous investigation^[14]. Shear texture is generally defined in terms of the crystallographic plane $\{hkl\}$ and the direction $\langle uvw \rangle$, aligned with the shear plane and the shear direction, respectively. For the ANZ, the zones from the top to the L-2.1 mainly contains B and \bar{B} components. While C, slight A_1^* and A_2^* components can be found at the middle positions (L-2.9, L-3.7). Besides, the predominant component of the bottom (L-4.5) is A. For the CNZ, B component is dominant within the zones from the top to the L-2.1. The intensity of A component also becomes weak at the bottom. For the RNZ, B and \bar{B} components can be detected at the positions from L-2.1 to L-2.9, whilst A and \bar{A} components are the major textures at the bottom positions (L-3.7, L-4.5). Therefore, it can be concluded that the texture distributions in the NZ are heterogeneous. Additionally, it is worth noting that the texture intensity in the middle of the NZ (L-2.1, L-2.9) is lower than that of the shoulder zone, which can be attributed to the stress and related complex material flow during the FSW^[15]. The chaotic flows in the middle of the joint could result in randomly oriented grains.

3 Conclusions

1) The NZ is mainly formed by the mixing agitation of the materials from the AS and RS. The materials mixing of the SAZ is not insufficient, while materials mixing mainly occurs in the middle of the NZ, accompanied by the presence of an onion ring.

2) The grain size of the NZ decreases from the top to the root. The fraction of dynamic recrystallization of the SAZ is lower than that of the middle of the NZ. The fraction of dynamic recrystallization decreases from the middle to the weld bottom.

3) Simple shear texture has been developed in the NZ, and the texture distribution is heterogeneous. The SAZ consists of B and \bar{B} components, while A or \bar{A} components are the major textures at the bottom position. C component is found in the middle of the NZ. Moreover, the texture intensity decreases first and then increases along the thickness direction from the top.

References

- Mishra R S, Ma Z Y. *Materials Science and Engineering R*[J], 2005, 50(1-2): 1
- Nandan R, DebRoy T, Bhadeshia H K D H. *Progress in Materials Science*[J], 2008, 53(6): 980
- Guo N, Fu Y, Wang Y et al. *Materials & Design*[J], 2017, 113: 273
- Peng Y Y, Yin Z M, Lei X F et al. *Rare Metal Materials and Engineering*[J], 2011, 40(2): 201
- Moradi M M, Aval H J, Jamaati R et al. *Journal of Manufacturing Processes*[J], 2018, 32: 1
- Suhuddin U, Mironov S, Sato Y S et al. *Materials Science and Engineering A*[J], 2010, 527(7-8): 1962
- Xu X, Lu Y, Zheng F et al. *Journal of Materials Engineering & Performance*[J], 2015, 24(11): 4297
- Imam M, Racherla V, Biswas K et al. *International Journal of Advanced Manufacturing Technology*[J], 2017, 91(5-8): 1753

- 9 Wang T, Zou Y, Matsuda K. *Materials & Design*[J], 2016, 90: 13
- 10 Wang B, Lei B, Zhu J et al. *Materials & Design*[J], 2015, 87: 593
- 11 Cho J, Kim W J, Lee C G. *Materials Science and Engineering A*[J], 2014, 597: 314
- 12 Xu W F, Liu J H, Chen D L et al. *Materials Science and Engineering A*[J], 2012, 548: 89
- 13 Canaday C T, Moore M A, Tang W et al. *Materials Science and Engineering A*[J], 2013, 559: 678
- 14 Fonda R W, Bingert J F. *Scripta Materialia*[J], 2007, 57(11): 1052
- 15 Yuan W, Mishra R S, Webb S et al. *Journal of Materials Processing Technology*[J], 2011, 211(6): 972

异种铝合金搅拌摩擦焊 AA2024-AA7075 接头沿厚度方向上的 EBSD 分析

张成行, 黄光杰, 曹 宇, 李 伟, 刘 庆

(重庆大学, 重庆 400044)

摘 要: 对 5 mm 厚的 AA2024-T351 和 AA7075-T651 铝合金板材进行搅拌摩擦对接焊, 采用电子背散射衍射 (EBSD) 法研究了异种铝合金搅拌摩擦焊 AA2024-7075 接头焊核区沿厚度方向的微观组织演化。结果表明: 焊核区的晶粒尺寸从焊缝顶部到底部依次降低。轴肩区和焊缝底部区域的再结晶组分低于焊缝中心区。焊核区形成了简单的剪切结构且结构分布不均匀。轴肩区主要是 B 和 \bar{B} 织构组分, 而底部区域主要是 A 和 \bar{A} 织构组分, C 织构组分则出现在中心区域。中心区域的织构强度低于焊核顶部和底部区域, 这主要是由于该区域出现了洋葱环, 是材料混合区域, 使得晶粒取向更为随机。

关键词: 铝合金; 搅拌摩擦焊; 微观组织; 织构

作者简介: 张成行, 男, 1992 年生, 博士生, 重庆大学材料科学与工程学院, 重庆 400044, 电话: 023-65112334, E-mail: chzhang@cqu.edu.cn